Activation of Hydrogen Peroxide in Horseradish Peroxidase Occurs within ~200 μs Observed by a New Freeze-Quench Device

Motomasa Tanaka,* Koji Matsuura,* Shiro Yoshioka,* Satoshi Takahashi,* Koichiro Ishimori,* Hiroshi Hori,† and Isao Morishima*

*Department of Molecular Engineering, Graduate School of Engineering, Kyoto University, Kyoto 606-8501, Japan; and †Division of Biophysical Engineering, Graduate School of Engineering Science, Osaka University, Toyonaka Osaka 560-8531, Japan

ABSTRACT To observe the formation process of compound I in horseradish peroxidase (HRP), we developed a new freeze-quench device with ~200 μs of the mixing-to-freezing time interval and observed the reaction between HRP and hydrogen peroxide (H_2O_2). The developed device consists of a submillisecond solution mixer and rotating copper or silver plates cooled at 77 K; it freezes the small droplets of mixed solution on the surface of the rotating plates. The ultraviolet-visible spectra of the sample quenched at ~1 ms after the mixing of HRP and H_2O_2 suggest the formation of compound I. The electron paramagnetic resonance spectra of the same reaction quenched at ~200 μs show a convex peak at $g = 2.00$, which is identified as compound I due to its microwave power and temperature dependencies. The absence of ferric signals in the electron paramagnetic resonance spectra of the quenched sample indicates that compound I is formed within ~200 μs after mixing HRP and H_2O_2. We conclude that the activation of H_2O_2 in HRP at ambient temperature completes within ~200 μs. The developed device can be generally applied to investigate the electronic structures of short-lived intermediates of metalloenzymes.

INTRODUCTION

Peroxidases are metabolizing heme enzymes that are distributed in fungal, plant, and mammalian organisms. The enzymes are involved in important physiological roles such as biosynthesis of hormones and stress and pathogen responses via the oxidation of various substrates at the expense of hydrogen peroxide (H_2O_2). The first step of the common catalytic sequence of peroxidases is the reaction between the ferric resting enzyme and H_2O_2. This reaction converts the enzyme into the two-electron oxidized species known as compound I, which has a ferryl oxo iron ($Fe^{4+}=O$) and a porphyrin π cation radical. Compound I oxidizes a substrate molecule to become the next intermediate, compound II, which returns to the resting state by oxidizing another substrate molecule (Dunford, 1991).

One of the unique characteristics of peroxidases is the rapid formation of compound I ($\sim 10^7$ M^{-1} s^{-1}; Dunford, 1991). Unlike peroxidases, oxygen-binding heme proteins such as myoglobin react with H_2O_2 slowly ($\sim 10^2$ M^{-1} s^{-1}) and do not form stable compound I (Matsui et al., 1999; Egawa et al., 2000). Poulos and Kraut (1980) proposed that the formation of compound I in peroxidases is promoted by the conserved His and Arg residues in the distal cavity of the heme. They assumed that the heme-peroxide complex called compound 0 was the precursor of compound I, whose O–O bond was cleaved with the aid of the distal His and Arg residues. Numerous mutagenesis studies verified the importance of these residues for compound I formation and supported the Poulus-Kraut model (Erman et al., 1993; Vitello et al., 1993; Newmyer and Ortiz de Montellano, 1995; Savenkova et al., 1998; Rodriguez-Lopez et al., 1996a,b, 2001).

Despite the accumulated evidence for the Poulus-Kraut model, the presence of compound 0 in peroxidases is suggested only by a few kinetic data including the low-temperature studies on horseradish peroxidase (HRP; Balny et al., 1987; Baek and Van Wart, 1989, 1992; Ozaki et al., 1998) and the study on the mutant of HRP (Rodriguez-Lopez et al., 1996b, 2001). The reaction between HRP and H_2O_2 at a cryogenic temperature indicates the saturation kinetics against the H_2O_2 concentration, which suggest the presence of an intermediate state before the formation of compound I (Balny et al., 1987; Baek and Van Wart, 1989, 1992). Baek and Van Wart further reported the low-temperature electronic absorption spectrum for the precursor, compound 0, which was later interpreted as the low-spin complex of heme with deprotonated peroxide anion (Baek and Van Wart, 1989, 1992; Harris and Loew, 1996). In contrast, the compound 0 species observed in the Arg-38→Leu (R38L) mutant of HRP is suggested as the high-spin complex of heme with neutral peroxide (Rodriguez-Lopez et al., 1996b, 2001). The low-temperature study that used polyethyleneglycolated HRP was rather consistent with the results of the R38L-mutant study (Ozaki et al., 1998). Thus, the properties of compound 0 that are suggested by these studies are not consistent.

A potentially powerful technique to characterize the kinetic and electronic properties of compound 0 is electron paramagnetic resonance (EPR) spectroscopy coupled with

Submitted May 28, 2002, and accepted for publication October 3, 2002.

Address reprint requests to Dr. Satoshi Takahashi or Prof. Isao Morishima, Dept. of Molecular Engineering, Graduate School of Engineering, Kyoto University, Kyoto 606-8501, Japan. Tel.: 81-75-753-5921; Fax: 81-75-751-7611; E-mail: st@mds.moleng.kyoto-u.ac.jp or morisima@mds.moleng.kyoto-u.ac.jp.

M. Tanaka's present address is Laboratory for Structural Neuropathology, Brain Science Institute, RIKEN, Wako, Saitama 351-0198, Japan.

S. Yoshioka's present address is Dept. of Biochemistry, Vanderbilt University, Nashville, TN 37232-0146.

0006-3495/03/03/1998/07 $2.00

the rapid-quenching method. This method has been utilized to characterize the intermediate states of various metalloenzymes since Bray (1961) reported the first application. The limitation of this technique, however, is the relatively long dead time. The time interval between mixing and freezing is ~5 ms, which is much longer than the estimated lifetime of compound 0 at room temperature. For example, the low-temperature results of Baek and van Wart (1989, 1992) can be extrapolated to room temperature to give a lifetime of ~1 ms. Accordingly, an improvement in time resolution is necessary for the rapid-quenching technique to be used for the characterization of compound 0.

To observe the reaction dynamics of HRP using EPR spectroscopy, we developed a new freeze-quench device that can interrupt chemical reactions within ~200 μs after mixing two solutions. Here we describe the design and performance of our device. The formation process of compound I in HRP was investigated using the device coupled with ultraviolet (UV)-visible and EPR spectroscopies. Our results demonstrate that the conversion of compound 0 to compound I is completed within ~200 μs at room temperature.

MATERIALS AND METHODS

Sample preparations

All chemicals were purchased from Wako (Osaka, Japan), Nacalai Tesque (Kyoto, Japan), and Dojindo (Kumamoto, Japan) as the highest quality available. The accurate concentration of H_2O_2 in a 30% (v/v) solution of H_2O_2 (Wako) was determined by a titration using potassium permanganate. Recombinant HRP isozyme C encoded in the T7 vector was expressed in *Escherichia coli* strain BL21 and extracted from the inclusion bodies as described previously (Tanaka et al., 1997). The activation of HRP by calcium and heme and the subsequent purification were conducted according to reported methods (Smith et al., 1990; Gazaryan et al., 1994) with some modifications (Nagano et al., 1996). The final RZ value was ~3.2. The concentration of HRP was determined by the Soret extinction coefficient of 103 mM^{-1} cm^{-1} (Paul et al., 1953). All solutions for spectroscopic measurements contained 50 mM 3-morpholinopropanesulfonic acid (MOPS) at pH 7.0 unless otherwise stated.

Construction of the rapid mixing and freezing device

All parts of the mixing and freezing device were homemade. A block diagram of the constructed system is depicted in Fig. 1. For the quenching experiments at ~200 μs (see Figs. 2, 3, and 6), the syringe pump was equipped with two 5-ml Hamilton syringes and supplied two solutions continuously at a flow rate of 4.2 ml min^{-1} per syringe. For the quenching experiments at ~1 ms (see Figs. 4 and 5), 5- and 1-ml syringes were utilized at flow rates of 2 and 0.4 ml min^{-1}, respectively. To reduce the sample waste, the sample solution was initially introduced into the sample loop (500 μl) and pushed by a buffer solution in the syringe (Fig. 1 *a*, syringe *S2*). The detailed design of the rapid mixer is indicated in Fig. 1 *b*. Two solutions were continuously introduced into the stainless mixing plate, which has a T-shaped mixing channel (Fig. 1 *b*, *circle*) that was drilled by Machida-Toolex (Tokyo, Japan). The plate was sandwiched by Teflon plates and tightened by metal blocks. The mixed solution flows through the exit channel (60-μm diameter; 200-μm length) and forms a jet.

The freezing device was composed of the rotating copper or silver disks and the liquid nitrogen dewar. The disks (2.5-cm diameter) were dipped in liquid nitrogen and rotated at the speed of ~1000 rpm. The rapid mixer was held at a distance of ~1 cm from the surface of the rotating disks, which were sprayed with the mixed solution. The frozen samples were transferred to liquid nitrogen during the rotation of the metal disks. After the freezing procedure, the powder samples were decanted and transferred manually to quartz cuvettes (1-mm inner thickness) or Suprasil tubes (4-mm inner diameter) immersed in liquid nitrogen for the optical absorption and EPR measurements, respectively. The sample powders were packed in the cuvettes or tubes, and the remaining liquid nitrogen was removed carefully. The procedures for the sample transfer were relatively easy due to the low viscosity and the specific gravity of liquid nitrogen. In contrast, the collection of sample powders from the isopentane bath was difficult and required a special technique (Tsai et al., 1998). To remove liquid oxygen from the EPR samples, the EPR tube containing the sample powders was moved to an isopentane bath cooled at ~150 K, evacuated using a vacuum line, and sealed. Great care should be practiced to prevent the potential hazard of accumulating liquid oxygen in the liquid nitrogen bath. We used a minimum amount of cooled isopentane, which was prepared and handled inside a draft chamber.

We initially utilized the copper disks for the freezing of sample droplets; however, we found that the copper disks occasionally gave cupric signals in the EPR spectra. We therefore used silver disks for the preparation of EPR samples. We confirmed that the copper and silver disks gave almost comparable time intervals between mixing and freezing. The samples quenched at ~200 μs (see Figs. 2, 3, and 6) and at ~1 ms (see Figs. 4 and 5) were prepared using the silver and copper disks, respectively.

Optical absorption spectroscopy

Optical absorption spectra were recorded on PerkinElmer spectrometer (Lambda 19). The spectrometer was modified to incorporate an Oxford cryostat (DN1704) at the sample compartment. To observe the spectra of powder samples, we inserted the frosted quartz plates in the sample and reference beams. Furthermore, the intensity of the reference beam was reduced using a black block to compensate for the intensity reduction of the sample beam. The sample temperature was monitored by a thermocouple inserted directly in the cell. The slit width and the scan rate of the spectrometer were adjusted at 2 nm and 120 nm min^{-1}, respectively. Although the inner thickness of the sample cells was 1 mm, the length should not be considered as the optical path length due to the powdery nature of the samples. The obtained spectra therefore reflect qualitatively the optical properties of the samples.

EPR spectroscopy

EPR spectra were measured on a Varian E-12 spectrometer equipped with an Oxford ESR-900 liquid helium cryostat. The microwave frequency was X-band (9.22 GHz), and the measurements were carried out with a modulation of 0.5 mT at 5 and 15 K. The microwave power was 5 mW.

RESULTS AND DISCUSSION

Design of the new freeze-quench device

There are two novel points in the design of the developed freeze-quench device. The first point is the utilization of the submillisecond mixing device that was originally developed by Regenfuss et al. (1985) and later redesigned by Takahashi et al. (1995, 1997). By using the mixer, we can achieve the mixing of two solutions within ~100 μs. Furthermore, due

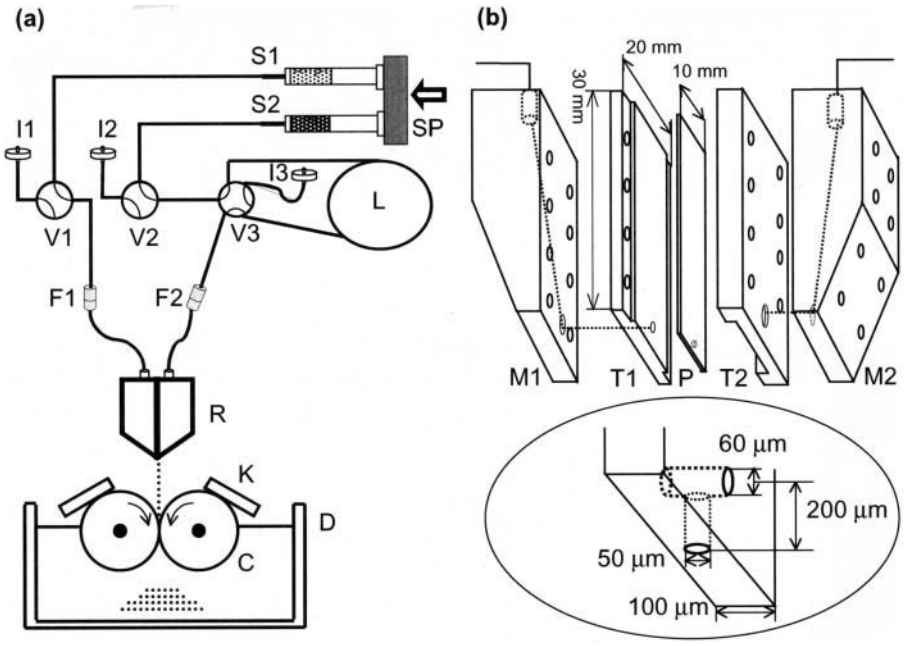

FIGURE 1 (*a*) A schematic diagram of the developed freeze-quench device. A solution of 8 mM H_2O_2 in 50 mM MOPS and a solution of 50 mM MOPS were introduced into two 5-ml syringes (*S1* and *S2*, respectively) through sample inlets with membrane filters (*I1* and *I2*). The syringe pump (*SP*) supplied the respective solutions continuously at a flow rate of 4.2 ml min^{-1} for each syringe. HRP (400 μM) dissolved in MOPS buffer was introduced in a sample loop (*L*) through an inlet (*I3*) and was pushed by the MOPS buffer from syringe S2. Flow valves (*V1*, *V2*, and *V3*) were used to control the sample flow. The H_2O_2 and HRP solutions were introduced into the rapid mixer (*R*) after they passed though in-line filters (*F1* and *F2*). The mixed solution was flushed against the rotating copper or silver disks (*C*) immersed in liquid nitrogen dewar (*D*). Polyethylene plates (*K*) were placed above the rotating disks to prevent the flow of liquid nitrogen over the rotating disks. (*b*) A close-up view of the rapid mixer. The two solutions were introduced into the stainless mixing plate (*P*) and mixed in the T-shaped channel drilled at the end of the plate as depicted in the circle. The plate was sealed with Teflon plates (*T1* and *T2*) and tightened by stainless blocks (*M1* and *M2*).

to the high mixing efficiency of the mixer, we can reduce the speed of sample supply (4.2 ml min^{-1} for each solution), which makes practical operation of the new device much easier than the conventional ram system (>30 ml min^{-1} for each solution).

The second novel point of the developed device is the utilization of the ''cold-block freezing'' method for freezing the mixed solution. Since the first report by Bray (1961), the rapid-quenching method for the spectroscopic application has been limited to the ''spray-freezing'' method, that is, spraying droplets of mixed solution into liquid cryogens such as cooled isopentane. However, it has been impossible to reduce the time interval between the mixing and freezing to <~5 ms using this method (Moodie et al., 1990; Saigo

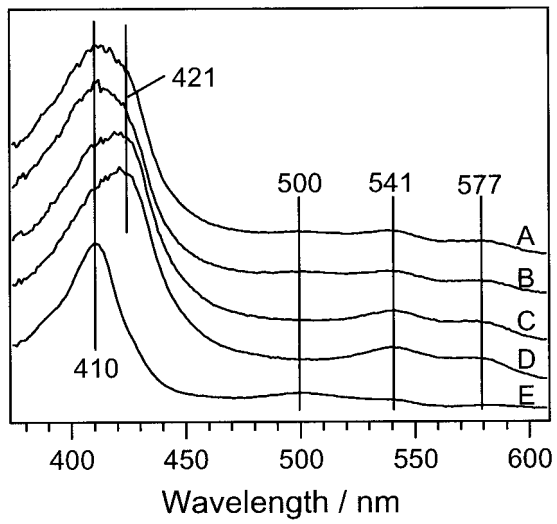

FIGURE 2 UV-visible absorption spectra of the reaction mixture between horse-heart myoglobin (100 μM) and azide (800 mM) prepared using the freeze-quench device. The spectra were recorded at 120 (*trace A*), 200 (*trace B*), 220 (*trace C*), and 240 K (*trace D*). The low-temperature absorption spectrum of metmyoglobin powder prepared using the freeze-quench device is also presented for comparison (*trace E*).

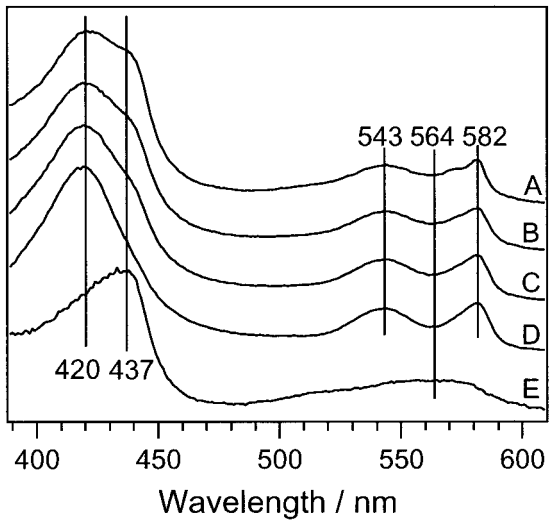

FIGURE 3 UV-visible absorption spectra of the reaction mixture between horse-heart myoglobin in the reduced form (100 μM) and oxygen (~140 μM) prepared using the freeze-quench device. The spectra were recorded at 130 (*trace A*), 200 (*trace B*), 210 (*trace C*), and 225 K (*trace D*). The low-temperature absorption spectrum of the ferrous form of myoglobin is also presented for comparison (*trace E*).

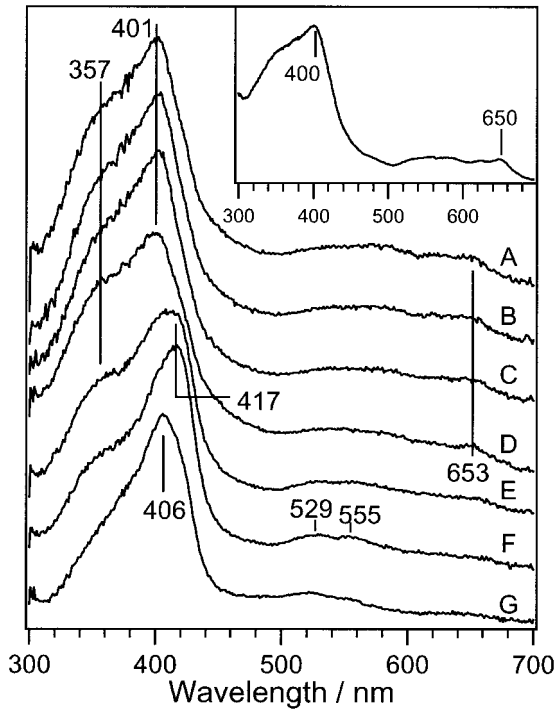

FIGURE 4 UV-visible absorption spectra of the reaction mixture between ferric HRP (20 μM) and H_2O_2 (400 μM) quenched within ~1 ms after mixing. The sample solution contained 50 mM MOPS adjusted at pH 7.0. The spectra were recorded at 114 (*trace A*), 160 (*trace B*), 202 (*trace C*), 230 (*trace D*), 246 (*trace E*), 256 (*trace F*), and 264 K (*trace G*). The spectrum of authentic compound I observed at room temperature is also shown (*inset*).

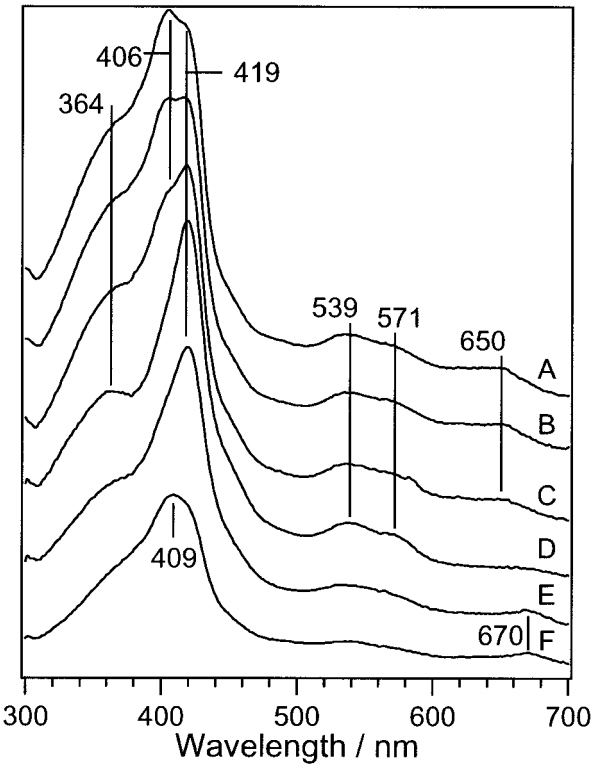

FIGURE 5 UV-visible absorption spectra of the reaction mixture between ferric HRP (60 μM) and H_2O_2 (10 mM) quenched within ~1 ms after mixing. The sample solution contained 50 mM sodium phosphate buffer adjusted at pH 7.0. The spectra were recorded at 150 (*trace A*), 200 (*trace B*), 220 (*trace C*), 230 (*trace D*), 260 (*trace E*), and 268 K (*trace F*).

et al., 1993). The rapid freezing of biological specimens has been studied extensively in the field of electron microscopy (Robards and Steytr, 1985). It is known that the fastest freezing time can be achieved by impacting a specimen onto the polished surface of cold metal blocks (cold-block freezing). For example, Bald (1985) estimated that the cooling rate of biological specimens placed on a cooled copper plate at 78 K was $>10^6$ K s^{-1} at 10 μm inside of the sample from the contact surface. Thus, small water droplets with a diameter of several tens of micrometers can be cooled >100 K within 1 ms after contact with cooled copper plates.

Freezing dead time of the freeze-quench device

The freezing dead time of the device was first estimated using a reference reaction between horse-heart metmyoglobin and azide. Two solutions that contained metmyoglobin and azide were injected into the freeze-quench device to final concentrations of 100 μM and 800 mM, respectively, at a rate of 4.2 ml min^{-1} for each solution. The UV-visible spectrum of the quenched sample was measured at 120 K (Fig. 2, *trace A*). A broad Soret band was observed at 413 nm, where the two Soret bands of metmyoglobin (410 nm for the frozen powers; Fig. 2, *trace E*) and azide-bound metmyoglobin (421 nm for the frozen powders; Fig. 2, *trace D*) were overlapped. The datum indicates that the device trapped the azide-binding reaction before its completion. Upon the increase in the sample temperature from 120 to 240 K, the Soret maximum gradually moved to 421 nm as shown in Fig. 2, traces B–D; this indicates the conversion to the azide-bound form. The changes in the absorption peaks in the visible region are also consistent with the conversion of metmyoglobin (500 nm) to the azide-bound form (541 and 577 nm). The disappearance of metmyoglobin demonstrates the perfect mixing of the two solutions before the freezing. We can roughly estimate that the amount of the azide-bound form in the spectrum taken at 120 K (Fig. 2, *trace A*) was ~50% via calculation of the spectral overlap of the azide-bound and free (Fig. 2, *traces D* and *E*, respectively) forms of metmyoglobin. Because the half-value period of metmyoglobin in the presence of 800 mM azide is ~120 μs at 21~23°C (Antonini and Burunori, 1971), the estimated dead time of the freeze-quench device is ~120 μs. We also confirmed that ~1 ms of the mixing-to-freezing time interval can be obtained by reducing the rates of sample supply to 0.4 and 2 ml min^{-1} for metmyoglobin and azide solutions, respectively (data not shown).

We further confirmed the mixing-to-freezing time interval using another fast reaction between myoglobin and oxygen. The reduced form of myoglobin (200 μM) in 50 mM MOPS

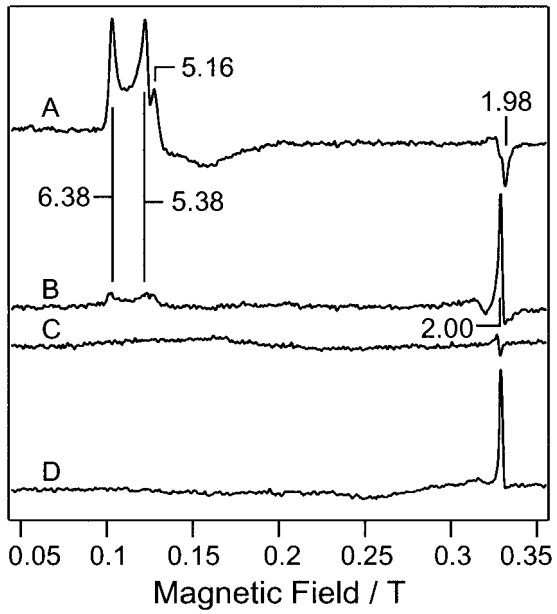

FIGURE 6 The EPR spectra of the reaction mixture between ferric HRP and H_2O_2 quenched within ~200 μs after the mixing. Trace A: the reference EPR spectrum for the ferric resting state of HRP (400 μM) in 50 mM MOPS buffer at pH 7.0 observed at 5 K. The sample was prepared by using the freeze-quench device. Trace B: the EPR spectrum for the reaction mixture between ferric HRP (400 μM) and H_2O_2 (8 mM) quenched at ~200 μs in MOPS buffer observed at 5 K. Trace C: the EPR spectrum for the reaction mixture between ferric HRP (400 μM) and H_2O_2 (8 mM) quenched at ~200 μs in MOPS buffer observed at 15 K. Trace D: the reference EPR spectrum for compound I of HRP prepared by manually freezing the mixture of HRP (310 μM) and H_2O_2 (400 μM) observed at 5 K. The interval between the mixing and freezing was ~30 s. The buffer solution was 50 mM MOPS at pH 7.0.

buffer at pH 7.0 was prepared using dithionite (~5 mM) and was anaerobically transferred to one of the syringes. The other syringe was filled with the same buffer saturated with air (~280 μM oxygen). Both solutions were injected into the freeze-quench device at a rate of 4.2 ml min^{-1}. Fig. 3, trace A indicates the optical absorption spectrum of the quenched sample at 130 K. Two Soret peaks at 437 and 420 nm indicate the presence of the ferrous deoxygenated (Fig. 3, *trace E*) and the ferrous oxygen-bound forms of myoglobin, respectively. The deoxy peak at 437 nm gradually disappeared upon the increase in the sample temperature to 200 K (Fig. 3, *trace B*), 210 K (*trace C*), and 225 K (*trace D*) and converted to the oxygen-bound form. These observations indicate that the device can mix two solutions completely and freeze the mixed solution before the completion of the oxygen binding to myoglobin. By calculating spectral overlap, we estimate the amount of the oxygen-bound form in the spectrum taken at 130 K was ~40%, which corresponds to ~200 μs of the time interval after the mixing of 140 μM oxygen at 20°C (Antonini and Burunori, 1971).

Although the determined time intervals between mixing and freezing should be considered as rough estimates, the two different reactions gave consistent time constants of 120~200 μs. We therefore conclude that the mixing-to-freezing time interval of the current device is ~200 μs. This is roughly an order shorter than those achieved by conventional techniques (~5 ms).

UV-visible spectra of the reaction mixture between ferric HRP and H_2O_2

Ferric HRP and H_2O_2 were mixed to final concentrations of 20 and 400 μM, respectively, and frozen ~1 ms after mixing using the developed freeze-quench system. We used 50 mM MOPS buffer adjusted at pH 7.0, because the buffer is known to be stable to the pH change at the low temperature (Orii and Morita, 1977). The UV-visible spectrum of the reaction mixture was measured at 114 K (Fig. 4, *trace A*) and showed a Soret absorption at 401 nm and a broad featureless band in the visible region. Notably, the spectrum at 114 K possessed a shoulder at 650 nm (Fig. 4, *inset*) that is characteristic of compound I (Dolphin et al., 1971; Dunford, 1991). The spectra suggest that the intermediate observed at ~1 ms is compound I.

We next examined the temperature dependence of the optical absorption spectra. The UV-visible spectrum of compound I was unchanged up to 202 K (Fig. 4, *traces B* and *C*), began to change at around 230 K (*traces D* and *E*), and at 256 K converted to a new species that has a Soret band at 417 nm and Q-bands at 529 and 555 nm (*trace F*). The spectrum is similar to that of compound II (419, 528, and 553 nm) when generated at room temperature and frozen by the developed device (spectrum not shown) and suggests the reduction of compound I to compound II at the higher temperature. The sample further indicates the change of the Soret maximum to 406 nm upon the increase in temperature to 264 K (Fig. 4, *trace G*), which is similar to that of the resting enzyme.

We noticed that the choice of buffer systems is important for obtaining consistent results at room and cryogenic temperatures. The same quenching experiment of the HRP-H_2O_2 reaction dissolved in a 50 mM sodium phosphate buffer was conducted. As indicated in Fig. 5 (*trace A*), the quenched sample within ~1 ms contained both compound I and compound II at 150 K as is evident from a peak at 650 nm and a shoulder at 419 nm. The latter feature grew as the temperature increased (Fig. 5, *traces B* and *C*). However, the visible peaks for compound II that were apparent at 230 K (Fig. 5, *trace D*) were observed at 539 and 571 nm, which are different from the peaks observed when the MOPS buffer was used (529 and 555 nm). A peak at 670 nm that appeared at 260 K (Fig. 5, *trace E*) suggests the modification of the heme macrocycle (Nakajima and Yamazaki, 1980) probably due to the high concentration (10 mM) of H_2O_2. We suggest that the fast formation and modified absorption spectrum of compound II that were observed in the phosphate buffer were caused by the pH change of the phosphate buffer at the

cryogenic temperature. Orii and Morita (1977) reported that the pH of sodium phosphate buffer can be decreased by ~4 units on freezing. Furthermore, an increase in the redox potential for the compound I/compound II couple at the low-pH condition was reported (Hayashi and Yamazaki, 1979). Thus, the low-temperature reaction of HRP in the phosphate buffer is modified from that at room temperature.

EPR spectra of the reaction mixture between ferric HRP and H_2O_2

To observe the faster phase of the reaction, we next quenched the sample at ~200 μs after mixing HRP and H_2O_2 in the MOPS buffer. Because it is difficult to differentiate compound I from the resting state by optical absorption spectra for powder samples, we examined the quenched sample using EPR spectroscopy. As shown in Fig. 6 (*trace B*), the EPR spectrum of the quenched sample observed at 5 K was characterized by a convex peak at $g = 2.00$. The convex signal at $g = 2.00$ was identical to the signal observed for compound I that was prepared by manually freezing the mixture of HRP and H_2O_2 in the MOPS buffer (the interval between mixing and freezing was ~30 s; Fig. 6, *trace D*). The convex peak disappeared upon the increase in temperature to 15 K (Fig. 6, *trace C*), which was in agreement with the relaxation broadening of the signal for compound I (Aasa et al., 1975; Schultz et al., 1979). Furthermore, the convex peak was not saturated up to 50 mW of microwave power (not shown), which was also in accordance with the signal of compound I (Aasa et al., 1975; Schultz et al., 1979). We conclude that the intermediate state observed in the quenched sample at ~200 μs is compound I. We also confirmed that the sample quenched at ~1 ms after being mixed in MOPS and phosphate buffers gave only the spectrum of compound I (not shown).

We could not observe signals from compound 0 in the quenched sample at ~200 μs. Previous studies revealed that the iron-peroxide complex of sperm whale myoglobin mutants, in which the distal His was replaced with Val or Gln, showed ferric low-spin signals at g values of 2.29, 2.16, and 1.91 (Brittain et al., 1997). On the contrary, the ferric high-spin state was proposed as the electronic state of compound 0 in the R38L mutant of HRP (Rodriguez-Lopez et al., 1996b). However, the small signals observed in the high-spin region ($g = \sim 6$) for the quenched sample (Fig. 6, *trace B*) arose from the remaining resting enzyme (*trace A*). The ferric low-spin hemes were also absent in the EPR spectrum observed at 15 K (Fig. 6, *trace C*), where the low-spin signals should be enhanced. The absence of even a trace amount of compound 0 at ~200 μs indicates that the lifetime of compound 0 at ambient temperature is <100 μs.

The current observation resolves conflicting information regarding the lifetime of compound 0. The low-temperature results by Baek and van Wart (1989, 1992) can be extrapolated to room temperature to give ~1 ms of the lifetime. In contrast, Balny et al. (1987) estimated ~20 μs from the similar low-temperature experiments. The discrepancy was likely caused by the difficulty in eliminating the artifacts of low-temperature experiments such as the pH changes of buffers as observed in this and previous studies (Orii and Morita, 1977). The destabilization of proteins in the methanol-based cryosolvents was also reported (Virden et al., 1990). The rapid-quenching method is free from these artifacts, because the reaction is initiated and conducted at room temperature in a normal buffer system. It is interesting to note that the estimated lifetime of compound 0 (<100 μs) is comparable with the timescale of O–O bond cleavage of dioxygen (O_2) conducted by cytochrome oxidase (~100 μs; Han et al., 2000). The structures surrounding the H_2O_2 or O_2 binding sites of these proteins should play essential roles in the very fast activation of the O–O bond. The distal structures were clarified in the atomic resolution for compounds I and II of HRP (Bergund et al., 2002). The kinetic and spectroscopic investigations on a submillisecond timescale using the developed device are important to comprehend the molecular mechanism of heme peroxidases and other metalloenzymes.

This work was supported by grant-in-aid 08249102 for scientific research on priority areas, ''Molecular Biometallics'' (to I. M.) from the Ministry of Education, Science, Culture, and Sports and by research fellowships of the Japan Society for the Promotion of Science for Young Scientists (to M. T.).

REFERENCES

Aasa, D., T. Vänngård, and H. B. Dunford. 1975. ESR studies on compound I of horseradish peroxidase. *Biochim. Biophys. Acta.* 391:259–264.

Antonini, E. and M. Burunori. 1971. Hemoglobin and Myoglobin In Their Reactions with Ligands. American Elsevier Publishing Co., New York.

Baek, H. K., and H. E. Van Wart. 1989. Elementary steps in the formation of horseradish peroxidase compound I: direct observation of compound 0, a new intermediate with a hyperporphyrin spectrum. *Biochemistry* 28:5714–5719.

Baek, H. K. and H. E. Van Wart. 1992. Elementary steps in the reaction of horseradish peroxidase with several peroxides: kinetic and thermodynamics of formation of compound 0 and compound I. *J. Am. Chem. Soc.* 114:718–725.

Bald, W. D. 1985. The relative merits of various cooling methods. *J. Microsc.* 140:17–40.

Balny, C., F. Travers, T. Barmann, and P. Douzou. 1987. Thermodynamics of the two step formation of horseradish peroxidase compound I. *Eur. Biophys. J.* 14:375–383.

Bergund, G. I., G. H. Carlsson, A. T. Smith, H. Szöke, A. Hendriksen, and J. Hajdu. 2002. The catalytic pathway of horseradish peroxidase at high resolution. *Nature* 417:463–468.

Bray, R. C. 1961. Sudden freezing as a technique for the study of rapid reactions. *Biochem. J.* 81:189–193.

Brittain, T., A. R. Baker, C. S. Butler, R. H. Little, D. J. Lowe, C. Greenwood, and N. J. Watmough. 1997. Reaction of variant sperm whale myoglobins with hydrogen peroxide. *Biochem. J.* 326:109–115.

Dolphin, D., A. Forman, D. C. Borg, J. Fajer, and R. H. Felton. 1971. Compounds I of catalase and horse radish peroxidase: π-cation radicals. *Proc. Natl. Acad. Sci. USA* 68:614–618.

Dunford, H. B. 1991. Horseradish peroxidase: structure and kinetic properties. *In* Peroxidases in Chemistry and Biology, Vol. 2. J. Everse, K. E. Everse, and M. B. Grisham, editors. CRC Press, Boca Raton, FL. 1–24.

Egawa, T., H. Shimada, and Y. Ishimura. 2000. Formation of compound I in the reaction of native myoglobins with hydrogen peroxide. *J. Biol. Chem.* 275:34858–34866.

Erman, J. E., L. B. Vitello, M. A. Miller, J. Wang, and J. Kraut. 1993. Histidine-52 is a critical residue for rapid formation of cytochrome *c* peroxidase compound I. *Biochemistry* 32:9798–9806.

Gazaryan, I. G., V. V. Doseeva, A. G. Galkin, and V. I. Tishkov. 1994. Effect of single-point mutations Phe41 → His and Phe143 → Glu on folding and catalytic properties of recombinant horseradish peroxidase expressed in *E. coli*. *FEBS Lett.* 354:248–250.

Han, S., S. Takahashi, and D. L. Rousseau. 2000. Time dependence of the catalytic intermediates in cytochrome *c* oxidase. *J. Biol. Chem.* 275:1910–1919.

Harris, D. L. and G. H. Loew. 1996. Identification of putative peroxide intermediates of peroxidases by electronic structure and spectra calculations. *J. Am. Chem. Soc.* 118:10588–10594.

Hayashi, Y. and I. Yamazaki. 1979. The oxidation-reduction potentials of compound I/compound II and compound II/ferric couples of horseradish peroxidases A2 and C. *J. Biol. Chem.* 254:9101–9106.

Matsui, T., S. Ozaki, E. Liong, G. H. Phillips, Jr., and Y. Watanabe. 1999. Effects of the location of distal histidine in the reaction of myoglobin with hydrogen peroxide. *J. Biol. Chem.* 274:2838–2844.

Moodie, A. D., R. H. Mitchell, and W. J. Ingledew. 1990. A gas-flow cryostat for use in freeze-quench studies: design and application to discontinuous pre-steady state spectral analysis. *Anal. Biochem.* 189: 103–106.

Nagano, S., M. Tanaka, K. Ishimori, Y. Watanabe, and I. Morishima. 1996. Catalytic roles of the distal site asparagine-histidine couple in peroxidases. *Biochemistry* 35:14251–14258.

Nakajima, R. and I. Yamazaki. 1980. The conversion of horseradish peroxidase C to a verdohemoprotein by a hydroperoxide derived enzymatically from indole-3-acetic acid and by *m*-nitroperoxybenzoic acid. *J. Biol. Chem.* 255:2067–2072.

Newmyer, S. L. and P. R. Ortiz de Montellano. 1995. Horseradish peroxidase His-42 → Ala, His-42 → Val, and Phe-41 → Ala mutants: histidine catalysis and control of substrate access to the heme iron. *J. Biol. Chem.* 270:19430–19438.

Orii, Y. and M. Morita. 1977. Measurement of the pH of frozen buffer solutions by using pH indicators. *J. Biochem.* 81:163–168.

Ozaki, S., Y. Inada, and Y. Watanabe. 1998. Characterization of polyethylene glycolated horseradish peroxidase in organic solvents: generation and stabilization of transient catalytic intermediates at low temperature. *J. Am. Chem. Soc.* 120:8020–8025.

Paul, K. G., H. Theorell, and A. Akesson. 1953. *Acta Chem. Scand.* 7:1284–1287.

Poulos, T. L. and J. Kraut. 1980. The stereochemistry of peroxidase catalysis. *J. Biol. Chem.* 255:8199–8205.

Regenfuss, P., R. M. Clegg, M. J. Fulwyler, F. J. Barrantes, and T. M. Jovin. 1985. Mixing liquids in microseconds. *Rev. Sci. Instrum.* 56: 283–290.

Robards, A. W. and U. B. Steytr. 1985. Low temperature methods in biological electron microscopy. *In* Practical Method in Electron Microscopy, Vol. 10. A. M. Glauert, editor. Elsevier, Amsterdam. 5–133.

Rodriguez-Lopez, J. N., D. J. Lowe, J. Heranndez-Ruiz, A. N. P. Hiner, F. Garcia-Canovas, and R. N. F. Thorneley. 2001. Mechanism of reaction of hydrogen peroxide with horseradish peroxidase: identification of intermediates in the catalytic cycle. *J. Am. Chem. Soc.* 123:11838–11847.

Rodriguez-Lopez, J. N., A. T. Smith, and R. N. F. Thorneley. 1996a. Recombinant horseradish peroxidase isoenzyme C: the effect of distal haem cavity mutations (His42 → Leu and Arg38 → Leu) on compound I formation and substrate binding. *J. Biol. Inorg. Chem.* 1:136–142.

Rodriguez-Lopez, J. N., A. T. Smith, and R. N. F. Thorneley. 1996b. Role of arginine 38 in horseradish peroxidase. A critical residue for substrate binding and catalysis. *J. Biol. Chem.* 271:4023–4030.

Saigo, S., H. Hashimoto, N. Shibayama, M. Nomura, and T. Nagayama. 1993. X-ray absorption spectroscopic studies of a transient intermediate in the reaction of cyanide metmyoglobin with dithionite by using rapid freezing. *Biochim. Biophys. Acta* 1202:99–106.

Savenkova, M. I., J. M. Kuo, and P. R. Ortiz de Montellano. 1998. Improvement of peroxidase activity by relocation of a catalytic histidine within the active site of horseradish peroxidase. *Biochemistry* 37:10828–10836.

Schultz, C. E., P. W. Devaney, H. Winkler, P. G. Debrunner, N. Doan, R. Chiang, R. Rutter, and L. P. Hager. 1979. Horseradish peroxidase compound I: evidence for spin coupling between the heme iron and a 'free' radical. FEBS Lett. 103:102–105.

Smith, A. T., N. Santama, S. Dacey, M. Edwards, R. C. Bray, R. N. F. Thorneley, and J. K. Burke. 1990. Expression of a synthetic gene for horseradish peroxidase C in *Escherichia coli* and folding and activation of the recombinant enzyme with Ca^{2+} and heme. *J. Biol. Chem.* 265:13335–13343.

Takahashi, S., Y.-C. Ching, J. Wang, and D. L. Rousseau. 1995. Microsecond generation of oxygen-bound cytochrome *c* oxidase by rapid solution mixing. *J. Biol. Chem.* 270:8405–8407.

Takahashi, S., S. R. Yeh, T. K. Das, C. K. Chan, D. S. Gottfried, and D. L. Rousseau. 1997. Folding of cytochrome *c* initiated by submillisecond mixing. *Nat. Struct. Biol.* 4:44–50.

Tanaka, M., K. Ishimori, M. Mukai, T. Kitagawa, and I. Morishima. 1997. Catalytic activities and structural properties of horseradish peroxidase distal His42 → Glu or Gln mutant. *Biochemistry* 36:9889–9898.

Tsai, A.-L., V. Berka, R. J. Kulmacz, G. Wu, and G. Palmer. 1998. An improved sample packing device for rapid freeze-trap electron paramagnetic resonance spectroscopy kinetic measurements. *Anal. Biochem.* 264:165–171.

Virden, R., A. K. Tan, and A. L. Fink. 1990. Cryoenzymology of Staphylococcal β-lactamase: trapping a serine-70-linked acyl-enzyme. *Biochemistry* 29:145–153.

Vitello, L. B., J. E. Erman, M. A. Miller, J. Wang, and J. Kraut. 1993. Effect of arginine-48 replacement on the reaction between cytochrome *c* peroxidase and hydrogen peroxide. *Biochemistry* 32:9807–9818.